The evolution patterns of temperature, pH, and voltage during the removal of chemical oxygen demand from a landfill leachate using electrocoagulation under different conditions

Rafiee, Poorya; Hosseini, Maryam; Ebrahimi, Sirous

DOI
10.1007/s11144-020-01846-0

Publication date
2020

Document Version
Accepted author manuscript

Published in
Reaction Kinetics, Mechanisms and Catalysis

Citation (APA)
Rafiee, P., Hosseini, M., & Ebrahimi, S. (2020). The evolution patterns of temperature, pH, and voltage during the removal of chemical oxygen demand from a landfill leachate using electrocoagulation under different conditions. *Reaction Kinetics, Mechanisms and Catalysis*, *131*(1), 319-334. https://doi.org/10.1007/s11144-020-01846-0

The evolution patterns of temperature, pH, and voltage during the removal of chemical oxygen demand from a landfill leachate using electrocoagulation under different conditions

Poorya Rafiee[1], Maryam Hosseini[2], Sirous Ebrahimi[1,3*]

[1]Biotechnology Research Centre, Faculty of Chemical Engineering, Sahand University of Technology, Tabriz, Iran

[2]Faculty of Chemical Engineering, Azarbaijan Shahid Madani University, Tabriz, Iran

[3]Department of Biotechnology, Delft University of Technology, Delft, Netherlands; s.ebrahimi@tudelft.nl

Abstract

In this study, electrocoagulation was evaluated for landfill leachate as a complex wastewater. Effects of all significant parameters including inter-electrode gap, current density, electrode material, time, pH, electrode numbers, salinity, and concentration were investigated. This study reports the changing patterns for chemical xxygen demand (COD) removal, temperature, voltage, and pH during EC for both Fe and Al electrodes under different conditions. According to the results, the best COD removals were achieved at shortest inter-electrode distance (0.5 cm), highest current density (1000 A m^{-2}), highest number of electrodes (6 plates), longest time (60 min), and within acidic pH. Furthermore, for different NaCl concentrations (0-16 g l^{-1}), both falling and rising patterns were observed. This study also provides separate results for the effect of operational parameters on pH, voltage, temperature, and energy consumption during EC. With higher inter-electrode distances, voltage and temperature rose to larger values, whereas pH fell. Besides, increases in initial pH caused rises in all voltage, temperature and pH parameters during EC. Experiments also displayed that higher values of voltage, temperature, and pH occurred at larger current densities. Additionally, with time, pH increased to more basic measures, and voltage similarly increased. Results also reported that although addition of NaCl into medium could drop the voltage and temperature, it formed both falling and rising patterns for pH at different NaCl concentrations. Plus, according to the results, voltage, temperature, and pH all experienced rising patterns in accordance with the increase in the number of electrodes. Finally, a comparative study of energy consumption was performed to analyse the operation parametric effect.

Key words: electrocoagulation, leachate, chemical oxygen demand, waste water treatment, removal efficiency, energy consumption

Introduction

Many attempts like reusing and recycling are adopted to reduce the amount of solid waste, while landfilling still remains the dominant method for the disposal of solid waste in many countries [1,2]. In addition, the produced leachate from landfilling embodies many environmental hazards for the pollutants it contains; namely persistent organic pollutants (POPs) and heavy metals. These complex compounds obviously complicate the treatment of landfill leachates [1]. The features of each leachate varies according to its waste style, age, climate, and perception condition [2]. Several methods have been applied for the treatment of landfill leachates, including biological, physiochemical, and membrane processes, each with their drawbacks hindering their application in the industry [1,2]. Chemical flocculation and coagulation remain important parts of water purification systems from raw and waste water due to their role in improving particle separation in subsequent processes [3]. Typical pollutants removed using chemical coagulation include nutrients, toxic heavy metals, and natural organic matter (NOM) [3]. Electrocoagulation (EC) is one of the widely-applied electrochemical techniques to treat wastewater and an advanced alternative to chemical coagulation [3]. As an independent or hybrid system, EC has been applied industrially to treat wastewater from textile dyes, pharmaceutical wastewater, oil tanning effluent, heavy metals, and other industrial wastewaters [4-9]. Electrocoagulation mainly consists of an electrolyte, usually the wastewater, and two sacrificial electrodes, anode and cathode. The reactions at the anode for Al and Fe electrodes are given by the following (1 [10]:

$$Al_{(s)} \rightarrow Al^{3+}_{(aq)} + 3e^- \quad E_0 = +1.66V \tag{1}$$

$$Fe_{(s)} \rightarrow Fe^{2+}_{(aq)} + 2e^- \quad E_0 = +0.44V$$

$$Fe_{(s)} \rightarrow Fe^{3+}_{(aq)} + 3e^- \quad E_0 = +0.04V$$

$$2Fe^{2+}_{(aq)} + 0.5O_{2(g)} + H_2O_{(l)} \rightarrow 2Fe^{3+}_{(aq)} + 2OH^-$$

Also, the reaction at the cathode is [10]:

$$2H_2O + 2e^- \rightarrow H_{2(g)} + 2OH^- E_0 = -0.83V \qquad (2)$$

Besides all advantages of EC, there are a few known drawbacks. One important disadvantage of EC is the formation of electrochemically generated compounds. For example, chlorinated organic compounds can form during the removal of organic compounds; or wastewaters containing high humic and fulvic acid contents can cause the formation of trihalomethanes [11]. Understanding the mechanisms involved in electrocoagulation can help resolve similar problems. In case of toxicity generation, for example, the toxicity and biodegradability assessments of electrocoagulated wastewater suggested shorter EC durations or the addition of another treatment stage based on a biological oxidation process [12,13]. The widely accepted theory for the involved mechanisms states that electrocoagulation consists of a series of stages: first, the metal ions are generated at the anode. Later, these ions form metal hydroxides and polyhydroxides which can later sweep the particles and cause them to settle (settlement). At cathode, water's simultaneous electrolysis produces small bubbles of oxygen and hydrogen at the cathode which in terms can float the particles at the surface of the medium (floatation). Then, the particles surface charges are destabilized causing them to approach to each other, aggregate, and form flocs (coagulation). Finally, chemical reactions and precipitation, including hydroxyl ions forming precipitate with particles, may occur [14,15].

Many investigations have successfully applied EC to remove COD from a landfill leachate [1,2,16-18]. In these studies, affecting parameters and their individual, and sometimes collective roles, in the enhancement of EC have been investigated. However, no study has focused on the parallel effect of each parameter on other parameters during the electrocoagulation. These parallel effects become remarkably significant when discussing pH, voltage, and temperature, all affecting the industrial operation costs: pH is adjusted through adding base or acids, voltage is the source of energy, and the temperature is controlled through cooling/heating. The significance of temperature stands out especially, since it has already been found that temperature can improve the COD removal [19].

In this study, the patterns for temperature, pH, and voltage were closely studied during the electrocoagulation of a landfill leachate for both Al and Fe electrodes at different pH values, EC durations, current densities, inter-electrode distances, electrode arrangements, and anion concentration values. Such patterns can help provide a better understanding of electrocoagulation mechanisms and economics. Finally, the energy consumption for each parameter was also calculated to compare the parametric influence on another significant economic factor.

Materials and Methods

Effluent

The landfill leachate was provided by Urban Landfill Leachate Disposal Organization, Tabriz, Iran. The initial characteristics of the wastewater are stated in Table 1-Initial characteristics of the experimental wastewater

.

Table 1-Initial characteristics of the experimental wastewater

Parameter	Value
COD (mg/l)	1928
TDS (g/l)	8.44
pH	7.94-8.34
color	Dark brown

Chemical oxygen demand determination

For each set of experiments, the chemical oxygen demand (COD) was measured before and after the electrocoagulation was run. COD analysis was performed according to Standard Methods for Examination of Water and Wastewater 5220-D [20]. Briefly, 2.5 ml of samples was taken and transferred into cells of spectrophotometer (Spectroquant, Merck -Germany) with screw caps of 16 mm. Each cell contained 3.5 ml of Ag_2SO_4 solution in concentrated H_2SO_4 and 1.5 ml of potassium dichromate solution. Then the combination of sample and reaction solution was transferred into thermoreactor and incubated at 148 °C for 2 hours. Consequently, the absorbance values were read at 600 nm against potassium biphthalate standard curve. If COD values of samples were lower than 100 mg l^{-1} the absorbance was read at the wavelengths of 420 nm.

Energy Consumption

The electrical energy consumption was calculated by Eq. 3:

$$E = VIt \quad (3)$$

Here E is the electric energy in Joule (J), V is the electric potential in volts (V), I is the electric current in amperes (A) and t is the time in seconds (s).

EC Cells

Electrocoagulation cells had a working volume of 250 ml each and were agitated by a magnet stirrer. Magnet stirrer was used to improve the mixing and enhance the charge transfer from electrodes to the medium at a faster rate. All experiments carried out at a constant current density of 500 A m^{-2}, provided by a DC power source (Dazheng, China), unless stated otherwise. All experiments were carried out for 15 min except the experiments in which the effect of time was to be investigated. The initial and final temperatures were measured using a mercury thermometer. pH values at the start and end of experiments were measured using a Consort Electrode (Belgium). Electrode materials included aluminium and mild steel with a total area of 0.004 m^2 for each pair.

Parameters

Inter-electrode distances of 0.5, 1, 1.5, 2, and 2.5 cm were applied to investigate the effect of electrode gap. In addition, current densities of 250, 750, and 1000 A m^{-2} were provided to the EC cells to evaluate the effect of current density. In these experiments, electrode gap was 0.5 cm. Concentrated NaOH and HCl (Merck, Germany) were used to set different pH values for the evaluation of pH effect. These pH set-points were decided based on the Pourbaix diagram of Fe to investigate the speciation of Fe, and Al set-points were set accordingly giving the pH values of 1.5, 4.2, 7.2, 9. It must be noted that the initial and final pH were measured at all experiments. According to preliminary results for pH tests (data not shown), when the initial pH is below 7 the pH change is between 2-3.5 units. However, the change within the 15 min of the experiment for pH values above 7 was between 0.2 and 1 pH unit. As a result, since the original pH for the leachate was about 8, no additional approach was taken to maintain a constant pH. To investigate the effect of time, samples were taken at the intervals of 3, 6, 8, 10, 15, 30, 45, and 60 min. To investigate the effect of number of electrodes, three sets of 2-plate, 4-plate, and 6-plate electrodes of both Al and Fe were selected and used. Bipolar arrangement was not studied, since there have been numerous reports on the better efficiency for monopolar over bipolar [21]. Finally, 1, 2, 4, 8, and 16 g l^{-1} of NaCl (Merck, Germany) were added to the wastewater and the mixture underwent EC to evaluate the effect of present anions in the electrolyte.

Results and Discussions

The effect of inter-electrode distance

pH evolution patterns in EC of Al and Fe electrodes with respect to inter-electrode distances are illustrated in Fig. 1a. According to Eq. 2, OH^- is constantly produced at cathode. Therefore, the pH has to increase with EC. With respect to the initial pH value of 7.96, such increase has occurred in all studied cases. However, the amount of this increase, varies in different cases. With an exception at 1.5 cm of inter-electrode distance for both electrode types, a descending pattern for pH values can be seen for all measured distances. This falling pattern can be explained by the length electrons have to cross to reduce water molecules at cathode. The more distant the electrodes are, the longer it takes for electrons to cross. Therefore, at more distant electrodes and for a fixed duration of EC, less electrons and consequently less hydroxide ions will be produced [22]. It can also be seen from Fig. ***1***a that Al pH values fall from Fe pH values. Standard electrode potentials for Al/Al^{3+} and Fe/Fe^{2+} are 1.66 and 0.44 V, respectively. These values show that Al electrode less readily loses electrons to form metal ions.

Fig. 1 Evolution patterns with respect to inter-electrode distance, at 500 A m^{-2} and 15 min for a) pH and COD removal b) voltage and temperature

Fig. 1a also shows the results from the removed COD versus different inter-electrode distances for both Al and Fe electrodes. The best results were obtained at the distance of 0.5 cm. Similar results were obtained in other EC studies [23]. It can be explained that with increasing the distance, a decrease in the amount of anode dissolution will occur, and the ions need to transfer a longer distance for the interaction to form flocs [24]. On the other hand, Fig. 1a shows a new rise to COD removal for gaps at 2 cm for Fe and Al electrodes. This means that at a point, with more distance, COD removal can increase similarly to other cases [24,25]. When the space between the electrodes is small, the electrostatic attraction between the electrode-generated ions causes constant collision with their counter-ions preventing them from forming flocs necessary for coagulation. However, at higher distances and at a constant current, resistance increases at more distant electrodes causing a drop in ion generation. Therefore, ion movement slows down which in terms permits enough time to form flocs [24].

Fig. 1b shows the evolution patterns of voltage and temperature with respect to inter-electrode distance. With increasing the distance, the ions need to transfer a longer distance for the interaction to form flocs [24]. On the other hand, at higher distances and a constant current, resistance increases at more distant electrodes for any given electrode length, causing a drop in ion generation. Therefore, ion movement slows down permitting enough time to form flocs[24]. A study has shown that for a distance and length ratio of electrode between 0.05 and 0.7, this relation between electrode gap and resistance is valid [26]. In the current study, with an electrode length of 8 cm, these ratios will perfectly fit in the range. In addition, according to Ohm's law, at constant current, with increasing resistance, voltage will naturally increase[27]. The results in **Error! Reference source not found.** confirm such understanding.

The obtained results from temperature evolution patterns versus inter-electrode distance are also depicted in **Error! Reference source not found.**. Results display a significant ascending pattern for both electrodes. Joule heating law confirms that with an increase in voltage, temperature increases [28]. Based on results from **Error! Reference source not found.**, temperature has to increase in both EC cells, since voltage increases with higher electrode distances. In most values from **Error! Reference source not found.**, Fe electrodes show a lower voltage consequently leading to a lower temperature. This observation agrees with similar studies [29] which can again be explained by Al's higher standard electrode potential compared to Fe's.

The effect of pH

Initial pH strongly influences the efficiency of EC process and therefore, the final pH values will differ accordingly. Successful mechanism of removal is due to AlO(OH) generation and FeO(OH) and Fe_3O_4 generations in case of Al and Fe electrodes [15]. Thus, to bring a sense of comparison, in Fig. 2a the difference between final and initial pH values have been compared. According to this figure, the pH difference (final pH minus initial pH) falls for both electrodes versus rising initial pH values. As for Al, hydrolyzed Al^{3+} ions generate the predominant complex $Al(H_2O)_6^{3+}$ at pH < 4. Increasing pH causes more hydrolysis of the complex and forming hydroxo complexes of aluminum such as $Al(OH)^{2+}$, $Al(OH)_3$, $Al(OH)^{4-}$, $Al_2(OH)_2^{4+}$, and $Al(OH)_5^{2-}$, and hydroxyl polymers such as $Al_{13}(OH)_{32}^{7+}$ from which only $Al(OH)_3$ is insoluble. Between pH of 5.2 and 8.8, $Al(OH)_3$, and above pH of 9, $Al(OH)_4^-$ are the predominant species [30]. Since $Al(OH)_3$ is the only insoluble species, it can be expected that at pH < 4 no hydroxyl ions must be consumed at the presence of only Al^{3+}. Later, with pH above 4 there must be an increase in pH, as many species will form from which only $Al(OH)_3$ is insoluble. This results in the remaining of most of the hydroxyl ions in the electrolyte and therefore increasing the pH. However, with pH more than 5.2, the amount of $Al(OH)_3$ formation will increase resulting in more and more hydroxyl consumption. Thus, a very sharp fall of pH is expected.

COD results in Fig. 2 confirm the pH effect, too. Within acidic pH predominant complexes of $Al(OH)_3$ are produced, while within basic pH the complexes become more soluble. Since $Al(OH)_3$ is the only insoluble species the best flocs must form around the pH of 5.2 and 8.8. The results state that the best values are obtained within the acidic pH for both Al and Fe electrodes. These results are in perfect agreement with previous studies [31,32].

Fig. 2 Evolution patterns with respect to initial pH, at 500 A m^{-2}, 15 min, and 0.5 cm electrode gap for a) pH and COD removal b) voltage and temperature

On the other hand, Pourbaix diagram of Fe [33] shows that for $pH < 4$, only Fe^{3+} and Fe^{2+}exist. In other words, no hydroxyl ions will be consumed from cathode to produce metal hydroxides. As a result, more hydroxyl ions will remain in the environment and pH will increase more relatively. For pH values between 4 and 9, Fe(III) hydroxide precipitates flocs with yellowish color, $Fe(H_2O)_3(OH)_3$. On the other hand, at $6 < pH < 9$, dark green Fe(II) hydroxide can also precipitate $Fe(H_2O)_4(OH)_2$[33]. In other words, with increasing pH, more hydroxide metals will form resulting in less hydroxyl concentration, and consequently less pH compared to lower pH values. Accordingly, COD, too, must be best removed within the pH values of 4 and 9 where there are precipitation of Fe(II) and Fe(III). The results in Fig. 2 clearly confirm such analysis. Another study also demonstrates that higher initial pH will linearly lead to higher final pH [2].

Subsequently, the relation between voltage and the different initial pH values was investigated and the results were depicted in **Error! Reference source not found.**. Nernst equation relates the reduction half-cell potential with the ion concentrations ((4) [34]:

$$E = E^0 - \frac{RT}{nF} ln \frac{(red)}{(ox)} \qquad (4)$$

Here E is the electrode potential (V), E^0 is the standard electrode potential (V), R is the gas constant, T is the absolute temperature (K), n is the number of involved electrons, F is the Faraday constant, and (red) and (ox) are the concentrations of reduced and oxidized species. At the room temperature of 25 °C, almost equal to experiments temperature of this study (23 °C), Nernst equation for reduction of iron to ferrous will be:

$$E = -0.44 + 0.012 \ln C_{Fe^{2+}} \qquad (5)$$

Here the concentration of Fe has been considered 1 for pure iron, and $C_{Fe^{2+}}$is the concentration of ferrous ion. Similarly, electrode potential for Al can be calculated as the following:

$$E = -1.66 + 0.008\ln C_{Al^{3+}} \tag{6}$$

Also, for the reduction of water to hydrogen and hydroxyl ions, the Nernst equation will be as follows:

$$E = -0.83 - 0.012ln\frac{{C_{H_2O}}^2}{P_{H_2}{C_{OH^-}}^2} \tag{7}$$

Here P_{H_2} is the hydrogen partial pressure. In dilute aqueous solutions, water has an overwhelming concentration, so it may be considered pure [35]:

$$E = -0.83 + 0.012\ln(P_{H_2}[OH^-]^2) \tag{8}$$

At the assumed temperature pOH can be replaced with pH and give:

$$E = -1.65 + 0.029\log(P_{H_2}) + 0.59pH \tag{9}$$

At constant hydrogen partial pressure, a linear relation between electrode potential and pH forms. The results in **Error! Reference source not found.** confirm such relation with R-values of 0.96 and 0.93 for Fe and Al electrodes, respectively (data not shown).

Error! Reference source not found. also shows the change in temperature with respect to initial pH values. A very slow ascending pattern can be seen for both electrodes, where temperature from an initial temperature of 23 increased to 28 and 31 °C for Fe and Al electrodes, respectively. These values later rose to 31 and 34 °C for pH 9. This rise, which is directly a result of increase in the voltage values, has already been observed. Comparing with Fe, higher temperature values for Al indicate higher voltage values.

The effect of current density

Next, the effect of current density was investigated on the patterns of voltage, temperature, and pH. As the results in Fig. 3 show there is a linear relation between pH evolution and the increase in current density. This linear relation can be explained by Faraday's law ((10) [36]:

$$m = \frac{ItM}{nF} \tag{10}$$

Here m is the electrode metal mass (g), I is the current (A), t is the EC duration (s), M is the molecular mass of the electrode material (g mol^{-1}), n is metal valence (2 for Fe and 3 for Al), and F is the Faraday constant (96500 C mol^{-1}). Naturally, with a higher current, and constant time, more metal ions, along with more electrons, will be produced at anode resulting in more hydroxyl production at the cathode. In other words, if all other terms in

(10 are kept constant, there will be a linear correlation between the current density and metal mass (or mole) which in terms can be correlated with its equivalent hydroxyl mass (or mol).

Fig. 3 Evolution patterns with respect to current density, at pH = 8 and 15 min for a) pH and COD removal b) voltage and temperature

Fig. 3 also illustrates how current density influences the COD removal. For both electrode types, increasing in current density led to an increase in removal efficiency. At the peak points, 43% and 45% of the COD were removed for electrode gap of 0.5 cm for Fe and Al electrodes at current density of 1000 A m^{-2}. The results showed that the current density linearly collaborates with the COD removal which is the direct result of Faraday's law. These results are in perfect agreement with the results from other studies on COD removal [2,16,37,38]. The higher the current goes; the more metal ions will be dissolved in the environment which will itself help both better neutralization of the colloidal charges and better metal hydroxides formation. In addition, the rate of bubble generation will increase, while the bubbles size will decrease, both improving the pollutant removal efficiency using electro-floatation [39].

Voltage pattern in accordance with current density change is shown in **Error! Reference source not found.**. It shows that at the Fe electrode gap of 0.5 cm, the current densities of 250, 750, and 1000 A m^{-2} led to voltages of 3.6, 8, and 13.5 V. Voltage values for Al electrode at the same electrode gap were 3.8, 9.1, and 13.2 V. For both electrodes, an obvious ascending pattern, due to the Ohm's law, can be seen. Another set of experiments were done at the electrode gap of 2 cm (data not shown) to obtain a better sense of these patterns at large and small inter-electrode gaps. Results for the same current density values and Fe electrode were 6, 13.1, and 21.8 V, and for Al electrodes were 6.8, 14.2, and 18.2 V. These values confirm the extra resistance added due to electrode distance gap, since voltages of 2-centimeter gap are higher in all cases compared to the electrode gap of 0.5 cm. The values for Al and Fe voltages are variably but comparably close to each other at the same current density and inter-electrode distance. The relative temperature pattern can be seen in **Error! Reference source not found.** as well.

The effect of time

Fig. 4 illustrates the results of voltage evolution versus duration of EC at a constant current density of 500 A m^{-2}. As the diagram shows, voltage increases for Al. Two mechanisms are widely accepted for electrocoagulation: denaturalization of colloidal ions and adsorption by metal hydroxides [40]. In both mechanisms, there is a consumption of ions. As a result, while time passes, with higher active ion removal due to EC, electrolyte activity decreases. Therefore, a higher voltage is necessary at the fixed current density. At the present work, with the passage of time, COD removal efficiency increased (**Error! Reference source not found.**). This is due to higher voltages presented in Fig. 4. A natural increase in temperature was expected due to longer time (data not shown). It must be noted that at a few points for both electrodes, a drop in efficiency is seen which can be explained by restabilization of the colloidal charge. The possibility of several destabilization and restabilizaion of colloids through dosing of coagulants has been fully discussed during a coagulation process elsewhere [41]. Similar mechanisms can be assumed for electrocoagulation as well.

Fig. 4 Evolution patterns with respect to EC time, at current density of 500 A m^{-2}, pH = 8, and inter-electrode gap of 0.5 cm for a) voltage b) pH and COD removal

According to (10, if all other terms are kept constant, there will be a linear correlation between the EC time and metal mass (or mole) which in terms can be correlated with its equivalent hydroxyl mass (mol). In accordance with EC time, this rise in pH values can be seen in **Error! Reference source not found.**.

The effect of anions

Addition of anions such as Cl^- can help the electrolyte power up to 30% [42]. Hence, with adding sodium chloride, the resistance and subsequently voltage are expected to fall. Results to investigate the effect of anion addition to voltage are depicted in Fig. 5. As expected, voltage decreased with respect to addition of more chloride. For Fe electrodes, the average voltage at 1 g l^{-1} added NaCl fell from the initial value of 8.5 to 4.9 V at 16 g l^{-1} added NaCl. For Al electrode, average voltage at 1 g l^{-1} added NaCl was 10.4 V which decreased to 5.4 at 16 g l^{-1} added NaCl. For a shorter inter-electrode distance of 0.5 cm (data not shown), the falling pattern repeated for both Al and Fe electrodes. However, the average voltages in both cases were smaller compared with 2 cm of inter-electrode distance. This can be explained by the additional reduction of electrical resistance caused by shorter distance between the electrode plates [22].

Fig. 5 Evolution patterns for with respect to added NaCl, at current density of 500 A m^{-2}, 15 min, and inter-electrode gap of 2 cm for a) voltage and temperature b) pH and COD removal

Following the voltage falling pattern, a falling pattern is expected for the temperature as well. These results, too, are illustrated in Fig. 5.

Error! Reference source not found. shows that a large drop in pH occurs at both Fe and Al electrodes after a certain concentration of NaCl. In electrolysis of aqueous sodium chloride, two half-reactions are possible at the cathode: reduction of water with standard potential of -0.83 V and reduction of sodium with standard potential of -2.71 V. It is obvious that water will be reduced due to its smaller standard potential. On the other hand, two half-reactions are similarly possible at the anode: oxidation of chloride and iron (or aluminum) ions with -1.36 V and 0.44 V (or 1.66 V). These values show that at dilute solutions of sodium chloride, iron converts to ferrous. However, with more concentrated NaCl solution, chloride gas will be produced at the anode and eventually ferrous ions will not be generated. Consequently, ferrous salts will not be formed and electrocoagulation will stop. These results were already confirmed by other studies [43]. These experiments were applied at 2 cm of electrode gap, and same pattern was achieved (data not shown).

The results of the other studies on the effect of NaCl on the medium are different. In one study, the COD removal for both Al and Fe electrodes showed a decline with increase in initial NaCl concentration interpreted as the formation of transitory compounds by Cl^- and $Al(OH)_3$ leading to a decrease in the amount of $Al(OH)_3$ coagulants [44]. However, in another study, the addition of NaCl led to improvement of the COD removal efficiency. The authors believed that active chlorine species concentration can improve the COD removal efficiency. Nevertheless, it must be noted that in the latter case graphite electrodes were used [45]. In the current study, while the EC with Fe electrode was almost fixed at COD removals of 31-37%, the Al-electrode electrocoagulation completely stopped at higher concentrations of NaCl. Apart from the decline in COD removal efficiency due to NaCl high concentrations, reaching a fixed trend after certain concentrations of NaCl has also been observed in another study [44].

The effect of electrode arrangement

The monopolar electrodes have the advantage of low voltage and high current [43]. The results of using monopolar arrangement for both Al and Fe electrodes have been compared. Two sets of 4-plate and 6-plate electrodes have been used to investigate the effect of number of electrodes. The evolution pattern for voltage with respect to number of electrode plates is illustrated in Fig. 6. An ascending pattern can be seen for the voltage. At constant current, the mean voltages for two-electrode modes were 6.9 and 7.5 V for Fe and Al electrodes, respectively. However, they increased to 12.3 and 11.1, for 4-plate system and 17.4 and 14.1 for 6-plate system, for Fe and Al electrodes. At a series arrangement of monopolar electrodes, equal current intensity flows through all electrodes, and a higher potential difference will be necessary [46]. Therefore, with an increase in number of the plates, more potential difference will be required to keep the current intensity constant through all electrodes.

Fig. 6 Evolution patterns with respect to number of plates, at current density of 500 A m^{-2} and 15 min for a) voltage and temperature b) pH and COD removal

Similar to previous conditions, high-voltage values fit with high-temperature values, therefore, making an ascending pattern for temperature as well (Fig. 6). Temperature increased from 29 °C at 2-plate to 33 and 42 °C for 4- and 6-plate Fe electrodes. EC final temperature for Al electrodes started at 35 °C for 2-plate experiment and rose to 42 and 47 °C for 4- and 6-plate experiments. However, as it can be seen in Fig. 6, Al electrodes show higher temperature, while Fe electrodes recorded higher voltage (Fig. 6).

Fe and Al, both, showed a rising pattern for pH along the increase of number of plates (**Error! Reference source not found.**). The rise in pH with respect to number of electrodes occurred at the fixed current density. At constant current density with 6 electrodes, more metal mass will dissolve compared to 2- and 4-plate experiments. As a result of more metal dissolution, more hydroxide ions will be produced leading to higher pH and also COD removal efficiencies.

Energy Consumption

An effective process must also be economically feasible including its electrical energy consumption. It has already been established that rising voltage in an electrocoagulation process will lead to a linear increase in electrical energy consumption [47]. As a result, every experiment which had a rising pattern for voltage did experience a rising pattern in energy consumption as well. For example, in case of the rising pattern as a result of higher electrode gaps (Fig. 1b), for Al electrodes, the energy increased from 11.7 kJ at 0.5 cm electrode gap to 18.18 kJ at 2.5 cm. These values for Fe electrodes were 14.94 and 18.9 kJ. Again, when the voltage increased at the experiments with different initial pH values, accordingly, the electrical energy rose from 7.2 kJ to 12 kJ between pH values of 1.5 and 9 for Fe electrodes. For Al electrodes, however, for similar pH intervals the energy consumptions started at 8.2 kJ and rose to 12 kJ (Fig. 2b). According to Fig. 3b, the rising current density formed a rising evolution for voltage as well. Thus, when both current and voltage increased, energy consumption sharply rose. For electrode gap of 0.5 cm, while for Al and Fe electrodes energy consumptions were measured to be 3.4 and 3.2 kJ at the lowest current density, they both dramatically moved up to 47.5 and 48.6 kJ. Similarly, with time proceeding and voltage growth (Fig. 4a), the energy consumption at Al electrodes, as expected, rose from 2.3 kJ at initial time to 93.6 kJ after 65 min. The electrical consumption for Fe electrode at this mode was not calculated. Interestingly, at a voltage falling pattern, like in anions addition (Fig. 5a), a falling pattern was also observed for electric energy consumption where it fell from 18.7 kJ at 1 g l^{-1} for Al electrodes to 9.7 kJ at 16 g l^{-1} NaCl concentration. Similarly, the energy consumptions for 1 and 16 g l^{-1} added NaCl were 15.3 and 8.8 kJ for Fe electrodes. Finally, in case of number of electrodes, the increase in voltage generated an increase in energy consumption (Fig. 6a). 4-plate and 6-plate Fe electrodes consumed 22.1 and 31.3 kJ electrical energy, whereas 19.9 and 25.3 kJ electrical energy was consumed for Al electrodes of the same numbers. The linear correlation between voltage and energy consumption has been also parametrically investigated in another study with similar results [48].

In a recent study to remove COD from a landfill leachate, sonication, electrocoagulation, and ozonization were used individually and also in collective hybrid systems where EC proved to be more efficient with almost 70% removal efficiency. Interestingly, they also reported higher removal efficiencies for hybrid systems including EC, too [48]. In the present study the highest removal efficiency was measured to be 47%. The main reason for this difference can be due to a much longer time (5 hours) in their work. In addition to COD removal efficiency, EC showed a much lower energy consumption (7.62 kWh m^{-3}) compared to sonication, ozonation, and their hybrid systems. It must be noted that, for optimization purposes, hey maintained the pH using additional acid and base, and improved the electrolyte by adding NaCl solution[48]. However, in the current study no additional substance was introduced into the medium. Plus, the contents and concentrations of wastewater differed. These collectively may be the reasons for the difference between the energy consumption between the two studies. Since the energy consumption was calculated to be 104 kWh m^{-3}.

Conclusion

In this study, a comprehensive investigation of different parameters was performed to monitor the four economic factors in industrial EC application: pH, temperature, voltage, and energy consumption. Obtaining the ascending/descending patterns for each of these factors along the operation will provide a better outlook on how far parameters like electrode gaps, initial pH, current density, etc. can go and the relation between these patterns and the COD removal efficiency can be better understood.

Acknowledgment

Authors would like to state their utmost gratitude to Urban Landfill Leachate Disposal Organization of Tabriz for providing the wastewater used in this study.

References

1. Huda N, Raman A, Bello M, Ramesh S (2017) Electrocoagulation treatment of raw landfill leachate using iron-based electrodes: effects of process parameters and optimization. Journal of environmental management 204:75-81

2. Tanyol M, Ogedey A, Oguz E (2018) COD removal from leachate by electrocoagulation process: treatment with monopolar electrodes in parallel connection. Water science and technology 77 (1):177-186

3. Vepsäläinen M, Sillanpää M (2020) Electrocoagulation in the treatment of industrial waters and wastewaters. In: Sillanpää M (ed) Advanced Water Treatment. Elsevier

4. Lakshmi PM, Sivashanmugam P (2013) Treatment of oil tanning effluent by electrocoagulation: Influence of ultrasound and hybrid electrode on COD removal. Separation and purification technology 116:378-384

5. Farhadi S, Aminzadeh B, Torabian A, Khatibikamal V, Fard MA (2012) Comparison of COD removal from pharmaceutical wastewater by electrocoagulation, photoelectrocoagulation, peroxi-electrocoagulation and peroxi-photoelectrocoagulation processes. Journal of hazardous materials 219:35-42

6. García-García A, Martínez-Miranda V, Martínez-Cienfuegos IG, Almazán-Sánchez PT, Castañeda-Juárez M, Linares-Hernández I (2015) Industrial wastewater treatment by electrocoagulation–electrooxidation processes powered by solar cells. Fuel 149:46-54

7. You HJ, Han IS (2016) Effects of dissolved ions and natural organic matter on electrocoagulation of As (III) in groundwater. Journal of environmental chemical engineering 4 (1):1008-1016

8. Song S, He Z, Qiu J, Xu L, Chen J (2007) Ozone assisted electrocoagulation for decolorization of CI Reactive Black 5 in aqueous solution: An investigation of the effect of operational parameters. Separation and purification technology 55 (2):238-245

9. Elnakar H, Buchanan IJJoEE (2020) Treatment of bypass wastewater using novel integrated potassium ferrate (VI) and iron electrocoagulation system. Journal of environmental engineering 146 (8):04020075

10. Mollah MYA, Schennach R, Parga JR, Cocke DL (2001) Electrocoagulation (EC)—science and applications. Journal of hazardous materials 84 (1):29-41

11. Mollah MY, Morkovsky P, Gomes JA, Kesmez M, Parga J, Cocke DLJJohm (2004) Fundamentals, present and future perspectives of electrocoagulation. Journal of hazardous materials 114 (1-3):199-210

12. Palácio SM, Espinoza-Quiñones FR, Módenes AN, Oliveira CC, Borba FH, Silva Jr FGJJoHM (2009) Toxicity assessment from electro-coagulation treated-textile dye wastewaters by bioassays. Journal of hazardous materials 172 (1):330-337

13. Manenti DR, Módenes AN, Soares PA, Boaventura RA, Palácio SM, Borba FH, Espinoza-Quiñones FR, Bergamasco R, Vilar VJJEt (2015) Biodegradability and toxicity assessment of a real textile wastewater effluent treated by an optimized electrocoagulation process. Environmental technology 36 (4):496-506

14. Rafiee P, Tong YW, Hosseini M, Ebrahimi S (2019) Electro-separation of microalgal culture from wastewater. Biocatalysis and agricultural biotechnology 22:101402

15. Darban A, Shahedi A, Taghipour F, Jamshidi-Zanjani AJCOiE (2020) A review on industrial wastewater treatment via electrocoagulation processes. Current opinion in electrochemistry 22: 154-169

16. Oumar D, Patrick D, Gerardo B, Rino D, Ihsen BS (2016) Coupling biofiltration process and electrocoagulation using magnesium-based anode for the treatment of landfill leachate. Journal of environmental management 181:477-483

17. Dia O, Drogui P, Buelna G, Dubé R, Ihsen BS (2017) Electrocoagulation of bio-filtrated landfill leachate: Fractionation of organic matter and influence of anode materials. Chemosphere 168:1136-1141

18. Li R, Wang B, Owete O, Dertien J, Lin C, Ahmad H, Chen G (2017) Landfill leachate treatment by electrocoagulation and fiber filtration. Water environment research 89 (11):2015-2020

19. Elnakar H, Buchanan (2020) Soluble chemical oxygen demand removal from bypass wastewater using iron electrocoagulation. Science of the total environment 706:136076

20. Baird RB, Bridgewater L, Clesceri LS, Eaton AD, Rice EW (2012) Standard methods for the examination of water and wastewater. American public health association,

21. Sahu O, Mazumdar B, Chaudhari P (2014) Treatment of wastewater by electrocoagulation: a review. Environmental science and pollution research 21 (4):2397-2413

22. Safwat SM, Hamed A, Rozaik EJSS, Technology (2019) Electrocoagulation/electroflotation of real printing wastewater using copper electrodes: A comparative study with aluminum electrodes. Separation science and technology 54 (1):183-194

23. Mameri N, Yeddou A, Lounici H, Belhocine D, Grib H, Bariou B (1998) Defluoridation of septentrional Sahara water of North Africa by electrocoagulation process using bipolar aluminium electrodes. Water research 32 (5):1604-1612

24. Khandegar V, Saroha AK (2012) Electrochemical treatment of distillery spent wash using aluminum and iron electrodes. Chinese journal of chemical engineering 20 (3):439-443

25. Aoudj S, Khelifa A, Drouiche N, Hecini M, Hamitouche H (2010) Electrocoagulation process applied to wastewater containing dyes from textile industry. Chemical engineering and processing: Process intensification 49 (11):1176-1182

26. Tobias CW, Wijsman R (1953) Theory of the effect of electrode resistance on current density distribution in electrolytic cells. Journal of the electrochemical society 100 (10):459-467

27. Millikan RA, Bishop ES (1917) Elements of electricity: a practical discussion of the fundamental laws and phenomena of electricity and their practical applications in the business and industrial world. American Technical Society

28. Von Meier A (2006) Electric power systems: a conceptual introduction. John Wiley & Sons

29. Ilhan F, Kurt U, Apaydin O, Gonullu MT (2008) Treatment of leachate by electrocoagulation using aluminum and iron electrodes. Journal of hazardous materials 154 (1-3):381-389

30. Gomes JA, Daida P, Kesmez M, Weir M, Moreno H, Parga JR, Irwin G, McWhinney H, Grady T, Peterson E (2007) Arsenic removal by electrocoagulation using combined Al–Fe electrode system and characterization of products. Journal of hazardous materials 139 (2):220-231

31. Un UT, Koparal AS, Ogutveren UB (2009) Electrocoagulation of vegetable oil refinery wastewater using aluminum electrodes. Journal of environmental management 90 (1):428-433

32. Akyol A (2012) Treatment of paint manufacturing wastewater by electrocoagulation. Desalination 285:91-99

33. Moreno-Casillas HA, Cocke DL, Gomes JA, Morkovsky P, Parga J, Peterson E (2007) Electrocoagulation mechanism for COD removal. Separation and purification technology 56 (2):204-211

34. Davis JR (2000) Corrosion: understanding the basics. ASM International

35. The Nernst Equation and Pourbaix Diagrams. https://www.doitpoms.ac.uk/tlplib/pourbaix/printall.php. Accessed 21 May 2017

36. Rajeshwar K, Ibanez J, Swain G (1994) Electrochemistry and the environment. Journal of applied electrochemistry 24 (11):1077-1091

37. Sridhar R, Sivakumar V, Immanuel VP, Maran JP (2011) Treatment of pulp and paper industry bleaching effluent by electrocoagulant process. Journal of hazardous materials 186 (2-3):1495-1502

38. Kobya M, Demirbas E, Akyol A (2009) Electrochemical treatment and operating cost analysis of textile wastewater using sacrificial iron electrodes. Water science and technology 60 (9):2261-2270

39. Daneshvar N, Ashassi-Sorkhabi H, Tizpar A (2003) Decolorization of orange II by electrocoagulation method. Separation and purification technology 31 (2):153-162

40. Comninellis C, Chen G (2010) Electrochemistry for the Environment, vol 2015. Springer

41. Bratby J (2016) Coagulation and flocculation in water and wastewater treatment. IWA publishing

42. Govindan K, Sumanasekara VD, Jang AJESWR, Technology (2020) Mechanisms for degradation and transformation of β-blocker atenolol via electrocoagulation, electro-Fenton, and electro-Fenton-like processes. Environmental science: Water research & technology 6 (5):1465-1481

43. Wang CT, Chou WL, Kuo YM (2009) Removal of COD from laundry wastewater by electrocoagulation/electroflotation. Journal of hazardous materials 164 (1):81-86

44. Elazzouzi M, Haboubi K, Elyoubi M (2019) Enhancement of electrocoagulation-flotation process for urban wastewater treatment using Al and Fe electrodes: techno-economic study. Materials today: Proceedings 13:549-555

45. Nidheesh P, Kumar A, Babu DS, Scaria J, Kumar MS (2020) Treatment of mixed industrial wastewater by electrocoagulation and indirect electrochemical oxidation. Chemosphere:126437

46. Fernandes A, Pacheco M, Ciríaco L, Lopes A (2015) Review on the electrochemical processes for the treatment of sanitary landfill leachates: present and future. Applied catalysis B: Environmental 176:183-200

47. Mohammadi MJ, Salari J, Takdastan A, Farhadi M, Javanmardi P, Yari AR, Dobaradaran S, Almasi H, Rahimi SJD, Treatment W (2017) Removal of turbidity and organic matter from car wash wastewater by electrocoagulation process. Desalination and water treatment 68:122-128

48. Asaithambi P, Govindarajan R, Yesuf MB, Selvakumar P, Alemayehu EJPS, Protection E (2020) Enhanced treatment of landfill leachate wastewater using sono (US)-ozone (O3)–electrocoagulation (EC) process: Role of process parameters on color, COD and electrical energy consumption. Journal of environmental management 204: 75-81

figure 1

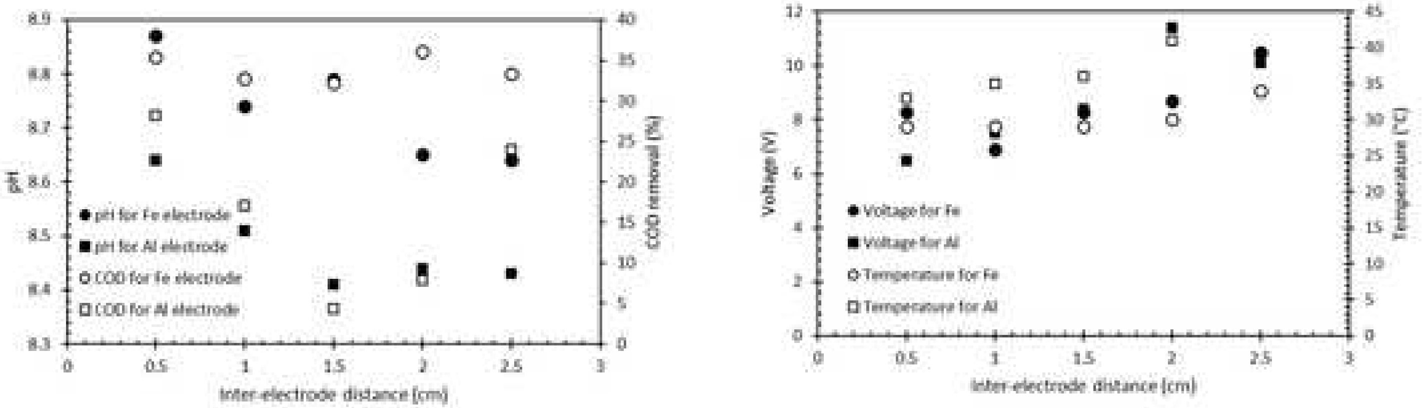
8.9
8.8
8.7
8.6
8.5
8.4
8.3
pH
0
0.5
1
1.5
2
2.5
3
Inter-electrode distance (cm)
40
35
30
25
20
15
10
5
0
COD removal (%)
● pH for Fe electrode
■ pH for Al electrode
○ COD for Fe electrode
□ COD for Al electrode
12
10
8
6
4
2
0
Voltage (V)
0
0.5
1
1.5
2
2.5
3
Inter-electrode distance (cm)
45
40
35
30
25
20
15
10
5
0
Temperature (°C)
● Voltage for Fe
■ Voltage for Al
○ Temperature for Fe
□ Temperature for Al

(a)

(b)

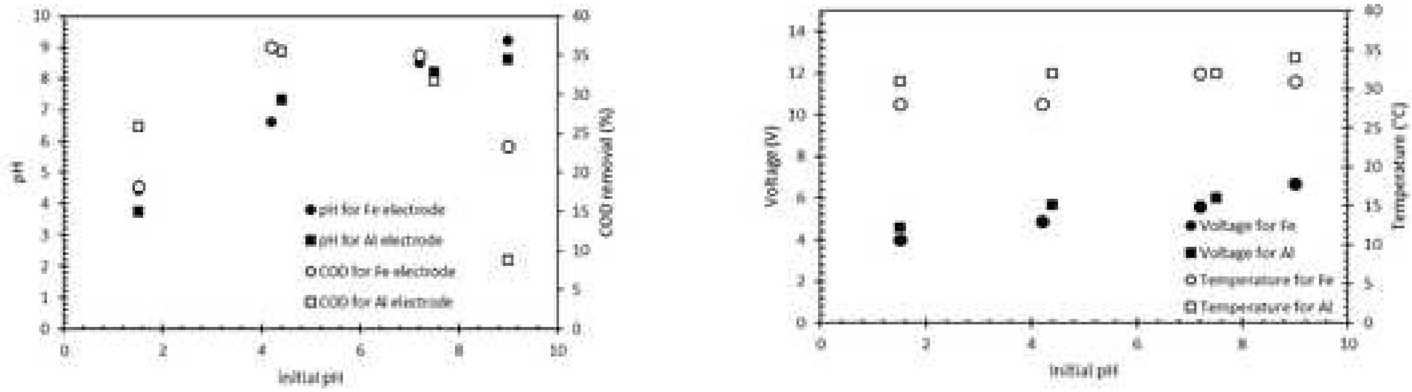
pH
0
1
2
3
4
5
6
7
8
9
10
COD removal (%)
0
5
10
15
20
25
30
35
40
Initial pH
0
2
4
6
8
10
● pH for Fe electrode
■ pH for Al electrode
○ COD for Fe electrode
□ COD for Al electrode
Voltage (V)
0
2
4
6
8
10
12
14
Temperature (°C)
0
5
10
15
20
25
30
35
40
Initial pH
0
2
4
6
8
10
● Voltage for Fe
■ Voltage for Al
○ Temperature for Fe
□ Temperature for Al

(a)

(b)

figure 3

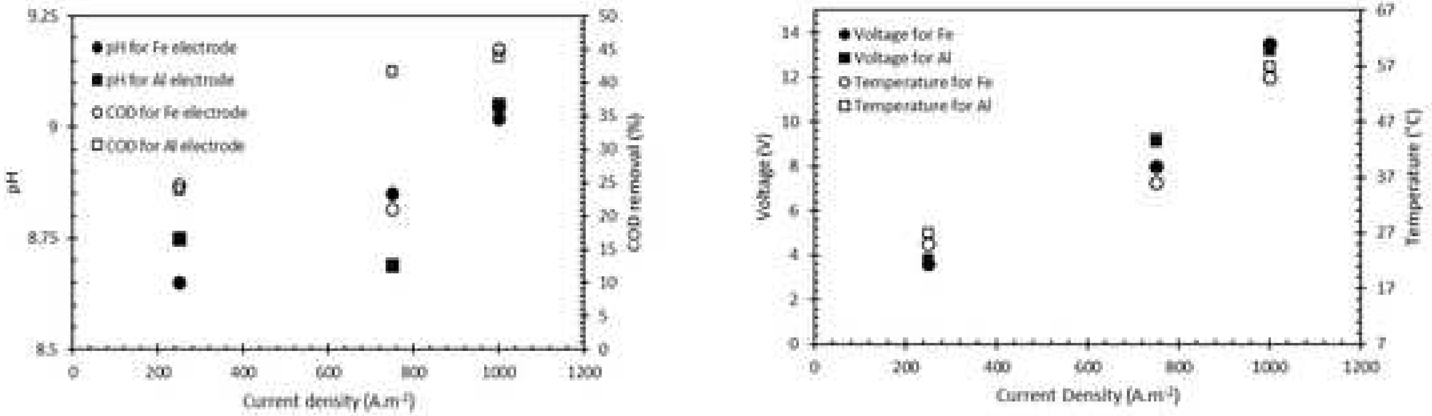
9.25
9
8.75
8.5
pH
● pH for Fe electrode
■ pH for Al electrode
○ COD for Fe electrode
□ COD for Al electrode
50
45
40
35
30
25
20
15
10
5
0
COD removal (%)
0
200
400
600
800
1000
1200
Current density (A.m⁻²)
14
12
10
8
6
4
2
0
Voltage (V)
● Voltage for Fe
■ Voltage for Al
○ Temperature for Fe
□ Temperature for Al
67
57
47
37
27
17
7
Temperature (°C)
0
200
400
600
800
1000
1200
Current Density (A.m⁻²)

(a)

(b)

figure 4

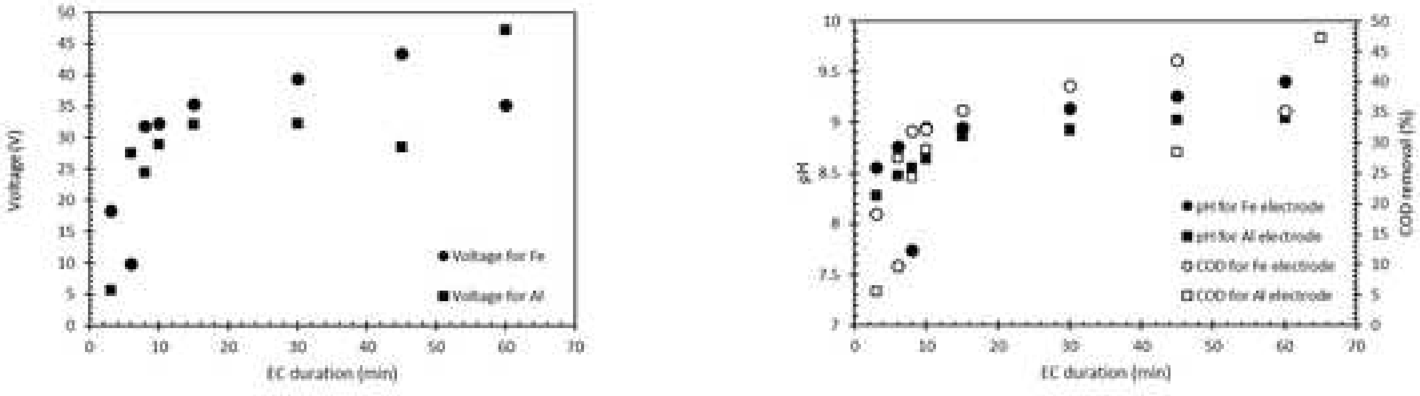
Voltage (V)
0
5
10
15
20
25
30
35
40
45
50
EC duration (min)
0
10
20
30
40
50
60
70
● Voltage for Fe
■ Voltage for Al
pH
7
7.5
8
8.5
9
9.5
10
COD removal (%)
0
5
10
15
20
25
30
35
40
45
50
EC duration (min)
0
10
20
30
40
50
60
70
● pH for Fe electrode
■ pH for Al electrode
○ COD for Fe electrode
□ COD for Al electrode

(a)

(b)

figure 5

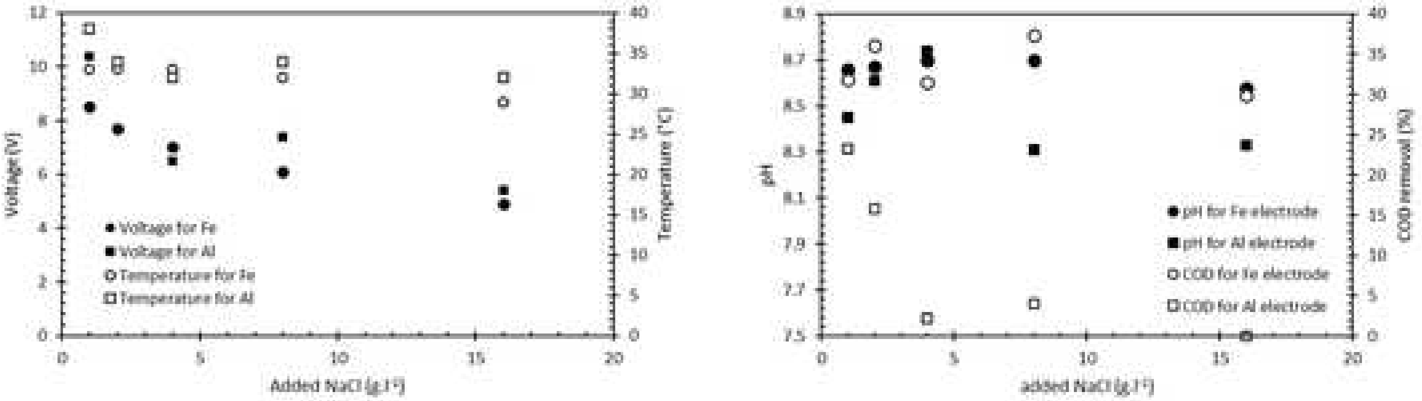
12
10
8
6
4
2
0
Voltage (V)
40
35
30
25
20
15
10
5
0
Temperature (°C)
0
5
10
15
20
Added NaCl (g.l⁻¹)
● Voltage for Fe
■ Voltage for Al
○ Temperature for Fe
□ Temperature for Al
8.9
8.7
8.5
8.3
8.1
7.9
7.7
7.5
pH
40
35
30
25
20
15
10
5
0
COD removal (%)
0
5
10
15
20
added NaCl (g.l⁻¹)
● pH for Fe electrode
■ pH for Al electrode
○ COD for Fe electrode
□ COD for Al electrode

(a)

(b)

figure 6

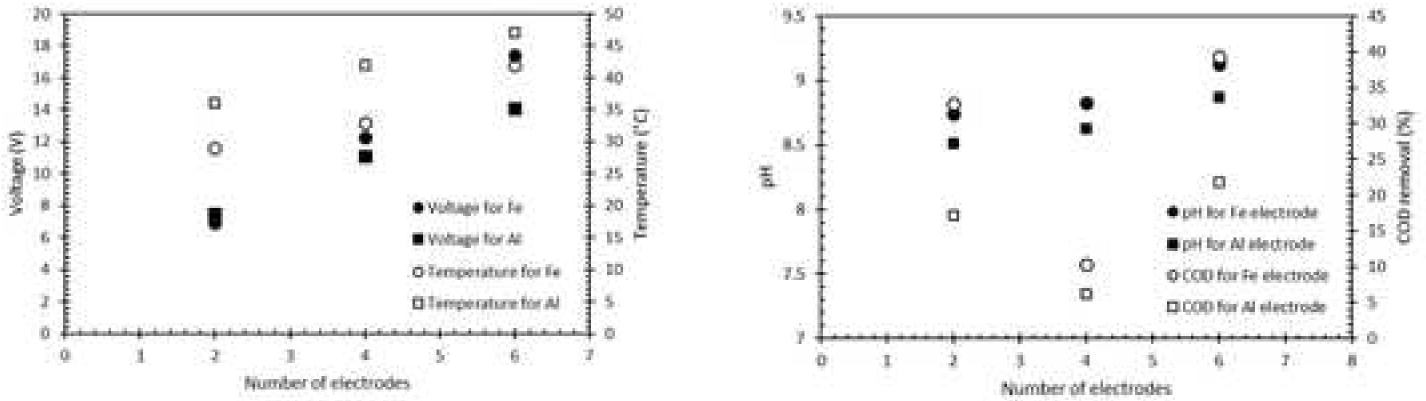
Voltage (V)
20
18
16
14
12
10
8
6
4
2
0
Temperature (°C)
50
45
40
35
30
25
20
15
10
5
0
0
1
2
3
4
5
6
7
Number of electrodes
● Voltage for Fe
■ Voltage for Al
○ Temperature for Fe
□ Temperature for Al
pH
9.5
9
8.5
8
7.5
7
COD removal (%)
45
40
35
30
25
20
15
10
5
0
0
1
2
3
4
5
6
7
8
Number of electrodes
● pH for Fe electrode
■ pH for Al electrode
○ COD for Fe electrode
□ COD for Al electrode

(a) (b)